Microstructural analysis of paper using synchrotron X-ray microtomography: numerical estimation of the permeability and effective thermal conductivity

SABINE ROLLAND DU ROSCOAT[1], MAXIME DECAIN[2], CHRISTIAN GEINDREAU[3], XAVIER THIBAULT[4] AND JEAN-FRANCIS BLOCH[5]

SUMMARY

Synchrotron X-Ray microtomography has already been successfully applied to visualise the inner structure of various grades of papers at a micron scale. The image analysis tools, previously developed, can provide quantitative data characterising the microstructures of papers. We studied two widely different samples - a Eucalyptus pulp handsheet and a commercial blotting paper. Numerical calculations were carried out on the tomography data to evaluate two specific physical properties - effective thermal conductivity and permeability.

The Representative Elementary Volume (REV) for each physical quantity considered, in terms of its 3 characteristic lengths in the three main directions, was defined by the respective correlation lengths (L_c).

Despite the small imaged volume (1400 µm x 1400 µm x paper_thickness), for any given property, whether microstructural or physical -:

- The REV characteristic lengths were similar for both samples,
- The REV was smaller than the imaged volume,

These results validate our approach and indicate that it may be extrapolated to other properties, for example, elastic properties.

KEYWORDS

Paper, microtomography, Representative Elementary Volume, microstructural property, permeability and effective thermal conductivity

[1]Post-Doctoral Researcher and corresponding author (srolland@esrf.fr), [4]Research Officer
European Synchrotron Radiation Facility,
6 Rue Jules Horowitz,
Polygone Scientifique
BP220, 38043 Grenoble, France

[2]PhD Student, [3]Professor
Laboratoire Sols-Solides-Structures-Risques
(3S-R / UJF / INPG /CNRS UMR 5521)
BP 53, 38041 Grenoble cedex 9, France.

[5]Professor
Laboratoire Génie des Procédés Papetiers
(LGP2/EFPG/CTP/CNRS UMR 5518),
BP 65, 38402 Saint-Martin-d'Hères Cedex, France

INTRODUCTION

Synchrotron X-Ray microtomography has already been successfully applied to visualise the inner structure of various grades of papers at a micron scale. The structures obtained are used to evaluate microstructural characteristics or to estimate numerically physical properties (*1*,*2*). Most of theses studies are based on the assumption of the existence of the Representative Elementary Volume (REV). The Representative Elementary Volume (REV) represents the smallest volume for which the mean value of a given physical quantity is equivalent to the one at the macroscopic size (usually a macroscopic length that characterises the sample at a macro-level at which the experience is carried out). The aim of this work is to define this REV, which , *a priori*, depends on the considered physical properties. It has to be emphasised that the determination of this REV is critical. Indeed, if this volume is not considered, the structural characterisations, or physical simulations, on a given volume, can not be extrapolated in the sense that they are not intrinsic. The results may depend for example on the considered size of the studied material or on the applied boundary conditions, which are necessary to solve numerically the physical considered problem.

The characteristic length L_{rev} of the REV has not been reported in previous works. It should satisfy the separation scale needed for homogenisation theory. We typically have $L_{micro} < L_{rev} << L_{macro}$ where L_{micro} and L_{macro} represents respectively the microscale and macroscale. In such a context, we want to ascertain if the data acquired are representative for different structural properties of the samples as the imaged volume is smaller (1400µm x 1400µm x paper_thickness) than the typical sizes of a paper sheet. In this case, it means that we have to evaluate the smallest representative elementary volumes. According to the typical size of a paper sheet, three scales can be considered for any microtomographic experiment: about 2mm (fibrous structure scale), 20mm (floc scale), 200mm (whole sheet scale).

This paper is dedicated to the determination of microstructural (porosity, specific surface area) and physical properties (effective thermal conductivity, permeability) of two paper samples acquired by Synchrotron X-Ray microtomography. These papers are a hardwood handsheet and a blotting paper. The evaluation of the REV is also discussed. As the REV is defined for a given property and for a given sample, it can be defined as the smallest volume that still represents the sample for a given characteristic with an estimated error. The REV size may be defined as a number of heterogeneity lengths (*3*,*4*). We apply this method to evaluate the REV for the following properties: porosity, specific surface area, effective thermal conductivity and permeability.

The paper is organised as follows: the first section presents the samples, the data acquisition systems and defines the heterogeneity length using the covariance diagram. The next section summarises the REV obtained for the microstructural properties - porosity and the specific surface area. Then the results concerning the physical characteristics - effective thermal conductivity and permeability are presented. These sections are followed by discussion and conclusion.

MATERIALS AND METHODS

Samples

We focus our attention on two paper samples that are a blotting paper and a hardwood handsheet denoted 'Blot' and 'Hard', respectively. These papers were chosen because they present different characteristics in term of paper making process, porosity and end-use properties. Neither sample contains fillers.

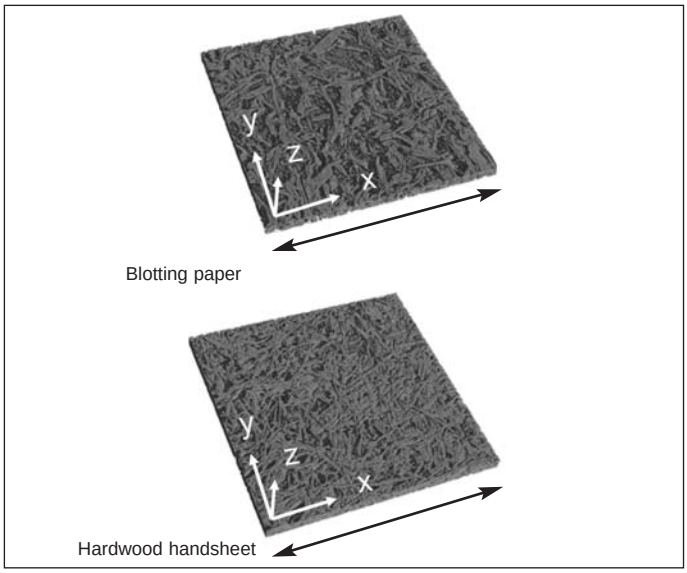

Fig. 1 3D visualisations of the studied samples: hardwood handsheet and blotting paper (700 µm x 700 µm x 35 µm)

Imaging technique and processing tools

Synchrotron Radiation microtomography in absorption mode is a technique widely used to describe the inner structure of the samples at a micrometric scale. Applied to paper samples, it gives relevant information on the 3D structure. In order to adequately define the microstructure of paper, a pixel size of 0.7 microns is chosen leading to a field of view of (1400 µm x 1400 µm x paper_thickness). The paper_thickness is about 110 µm and 550 µm for 'Hard' and 'Blot', respectively. To obtain quantitative measurements on the microstructure, image processing tools were developed and applied to binarise the structure (*5*). Figure 1 presents 3D views of these two samples. This figure shows that the long axes of most of the fibres are almost parallel to the plane (*x*,*y*). Thus, these microstructures are close to orthotropic. Moreover the paper 'Hard' which only contains hardwood fibres seems to be homogeneous. On the 3D images of the paper 'Blot', we can distinguish both hardwood fibres (small fibres) and softwood fibres (large fibres).

Covariogram

The microstructure of both paper samples is anisotropic. This anisotropy is illustrated by 2 slices of the microstructure within the 2D planes (x,y) and (x,z) respectively (Fig. 2).

To quantify this observation, the covariances are evaluated in the main directions x, y and z from images. The covariance function of the set X is the probability for the two points s and s + h to be in the set X where *h* represents a translation. This function has the following properties for a random set (*6*). It is equal to the set porosity when *h* is null and tends to an asymptotic value when h tends to infinity. Notice that the covariance is equal to the porosity when h is null. Figure 2 illustrates the covariograms obtained in the two main planes (x,y) and (y,z) for the 'Blot' paper. First we can notice that the covariance is equal to the porosity of the considered slice when *h* is null. We can also observe that the covariance reaches an asymptotic value equal to the square of porosity for a finite range Lc. Lc_x and Lc_y present similar values indicating an isotropic structure within the plane (x,y). Lc_z is much smaller. This confirms the visual observation that the 3D microstructure is orthotropic. These lengths characterise the size of heterogeneities in a given direction. This is illustrated in the case of the blotting paper (Fig. 2) but we find similar results in the case of the handsheet. Both samples present a value of Lc_z of about 3 microns in the thickness direction. Lc_x (or Lc_y) is about 33 microns and 26 microns for 'Hard' and 'Blot', respectively. The

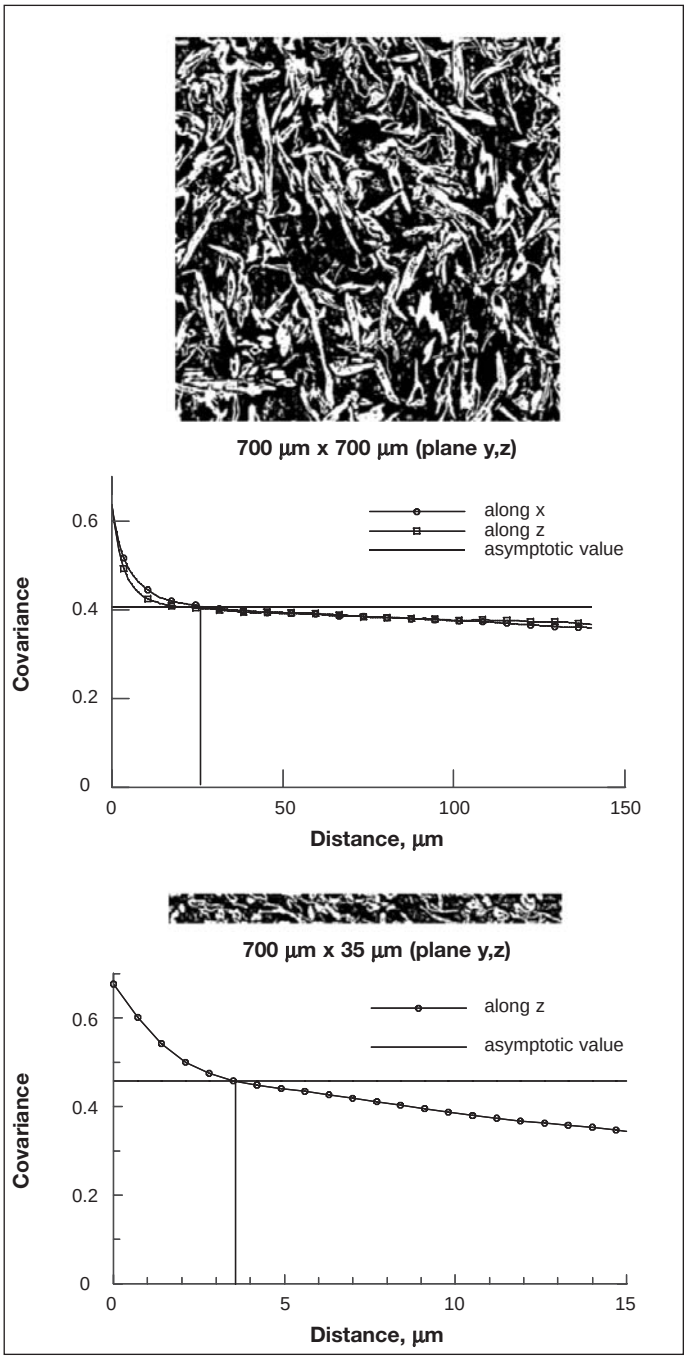

Fig. 2 Blotting paper: In-plane (top) and thickness (bottom) slices and their corresponding covariograms.

anisotropy of both microstructures may be characterised by the ratio Lc_x/Lc_z (or Lc_y/Lc_z). This ratio is approximately 12.4 and 7.4 for 'Hard' and 'Blot', respectively.

Porosity profile and bulk definition

If we study the porosity profiles in the thickness direction of both samples (Fig. 3), we can notice that both profiles have similar shapes: a decrease in porosity at the top surface, a plateau and finally an increase in porosity at the bottom surface. The plateau corresponds to the bulk whereas the two varying parts can be related to the surface layers.

The porosity obtained on microtromographic data corresponds to one measured by standards. Notice that porosity is smaller in the bulk for both samples. Therefore we would like to investigate the representativity of the imaged volume as it is small compared to the typical sizes of a paper sheet.

Method for REV evaluation

In this paper, we restrict the evaluation to the REV of structural and physical properties in the bulk. To estimate the REV, we evaluate the properties of interest (porosity, specific surface area, effective thermal conductivity, permeability) for larger and larger volumes chosen in the bulk always centred on the same voxels (*7*). The sizes studied were (L x L x 35 µm) where L represents the side (size) of the volume within the plane (x,y) (Fig. 1).

This length L varies from 50 µm to 700 µm. The thickness of the volume remains constant and equal to 35 µm. The influence of this size on the results will be discussed later. The REV size is then defined as the size (L x L x 35 µm) of a volume, beyond which the effective quantity studied becomes more or less constant. We will show that the characteristic length of the REV depends on the property and can be linked to the heterogeneity length (Lc_x or Lc_y), as suggested in (*3,4*). The results are presented in the following sections.

Table 1
Comparison between classical measure and tomographic results for porosity for both samples.

(%)	Exp. results	Tomo. results: whole sample	Tomo results: bulk
Hard	60	57	53
Blot	66	71	64

MICROSTRUCTURAL PROPERTIES AT THE SAMPLE SCALE

Porosity

The porosity can be evaluated on binarised data by the ratio of voxels belonging to the pore phase to the whole number of voxels. Figure 4 shows the evolution of porosity as a function of the length L We can observe that the porosity tends to an asymptotic value when the length L of the volume is larger than 400 µm. This length is about 14 times the heterogeneity length Lc_x (or Lc_y). The REV is also linked to a relative error. To evaluate it, we consider the obtained property in the whole bulk (1000 µm x 1000 µm x bulk_thickness) as a reference. Therefore for a volume (L x L x 35 µm) where L = 10 Lc_x, the relative error made on porosity measurement is around 3.6% for the 'Blot' paper and 4.3% for the handsheet. This volume (10 Lc_x x 10 Lc_y x 35 µm) is smaller than the total bulk volume (1000 µm x 1000 µm x 35 µm) and much smaller than the field of view (1400 µm x 1400 µm x paper_thickness).

Specific surface area

Using stereological tools, we have evaluated the specific surface area (*4*). The results are presented in the following (Fig. 5) in a dimensionless form, divided by an arbitrarily chosen value of 1.2 x 10^5. In a similar way to porosity, we can observe that the specific surface area tends to an asymptotic constant value when the length L of the volume is larger than 400 µm (about 14 Lc_x or Lc_y). Once again we consider the dimensionless specific surface area of the whole bulk as reference. Therefore if we consider a volume (10 Lc_x x 10 Lc_x x 35 µm), the relative error made on specific surface area measurement is 9.9 % and 1.3 % for 'Blot' and 'Hard, respectively.

These results show that

i) the REV sizes for the porosity and the specific surface area are of the same order of magnitude (10 Lc_x x 10 Lc_x x 35 µm), and
ii) the volume imaged is sufficient to estimate both the microstructural properties.

NUMERICAL ESTIMATION OF PHYSICAL PROPERTIES

We now focus our attention on two physical properties of both paper samples - the effective thermal conductivity and the permeability. These properties have been estimated by solving numerically, on dif-

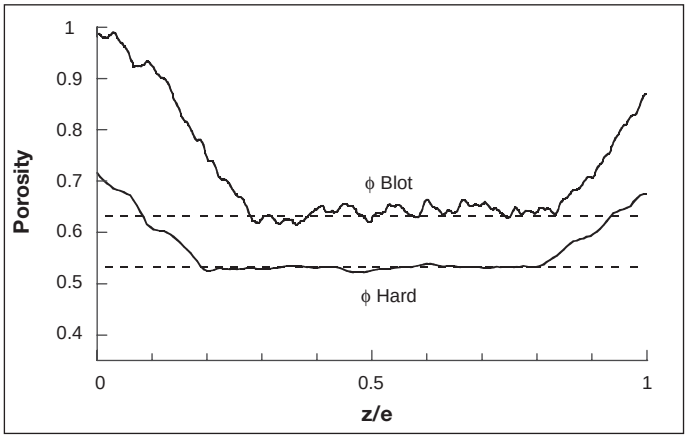

Fig. 3 Porosity profiles along the normalized thickness of the whole sample (1000 µm x 1000 µm) for the 2 papers (plain lines) and mean porosity in the bulk (dashed lines).

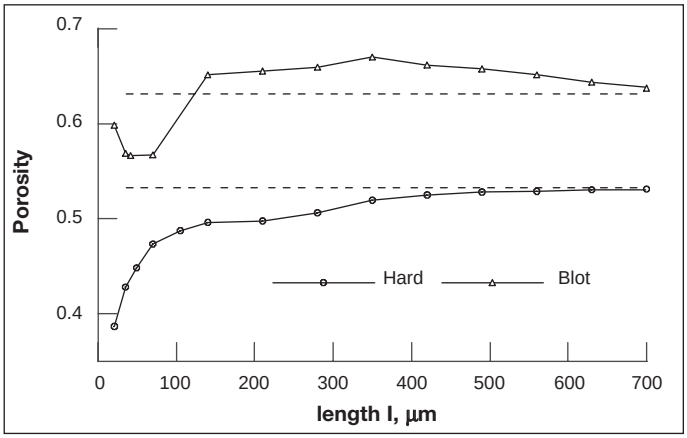

Fig. 4 Evolution of the porosity versus the (size) side L of the volume (L x L x 35 µm^3) for both studied papers. Dash lines represent the mean porosity in the 'bulk' layer for each paper.

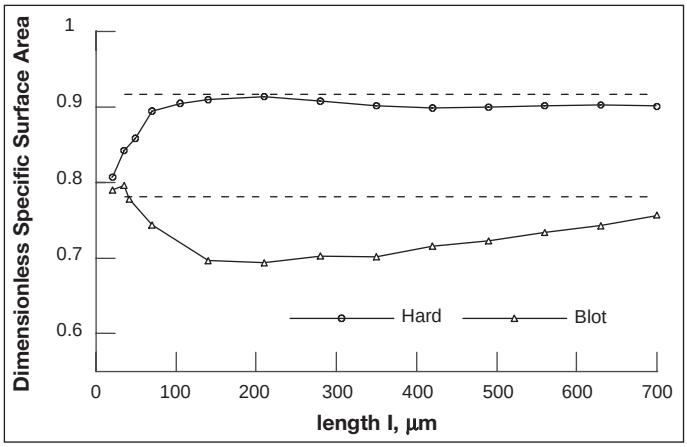

Fig. 5 Evolution of the dimensionless specific surface area versus the (size) side L of the volume (L x L x 35 µm³) for both studied papers. Dash lines represent the mean porosity in the 'bulk' layer for each paper.

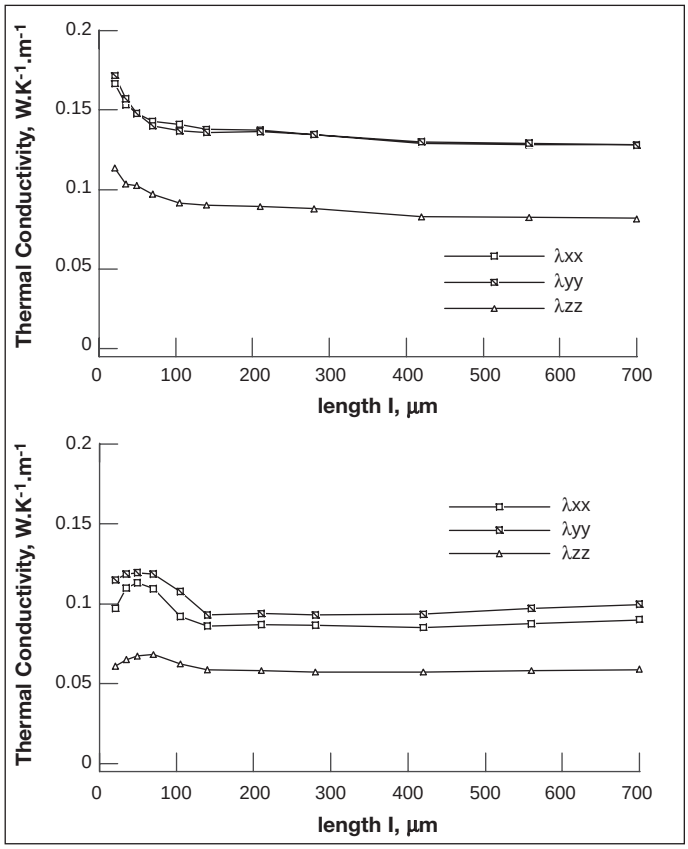

Fig. 6 Evolution of the diagonal components of the effective thermal conductivity tensor versus the (size) side of the volume (L x L x 35 µm³) in the bulk for 'Hard' (top) and 'Blot' (bottom).

ferent volumes, specific boundary value problems arising from the homogenization process. These boundary value problems are not reproduced here but can be found elsewhere (*8,9*). They have been solved by using finite volume software packages (*9,10*). As for the microstructural properties, the effective thermal conductivity and the permeability of the bulk of each paper have been computed on volumes (L x L x 35 µm), where L varies from 50 µm to 700 µm. The REV size for both physical properties is estimated and compared with the one obtained for microstructural properties.

Thermal properties

The two samples contain only two phases, pores and fibres, whose intrinsic thermal conductivities are 0.026 and 0.33 $W.K^{-1}.m^{-1}$, respectively. These intrinsic thermal conductivities are assumed to be isotropic.

Figure 6 presents the evolution of the diagonal components of the effective thermal conductivity tensor of both samples versus the length L of the volume. The non-diagonal components of the effective thermal conductivity tensor are negligible and therefore not presented here.

It can be observed that the effective thermal conductivities λ_{xx} and λ_{yy} are of the same order of magnitude whereas the transversal one, λ_{zz} is much smaller. These results show that the effective thermal conductivity tensor is transverse isotropic, similar to the microstructure. The anisotropy for the effective thermal conductivity may be defined as the ratio $\lambda_{xx}/\lambda_{zz}$ (or $\lambda_{yy}/\lambda_{zz}$). This ratio is approximately 1.55 for both 'Hard' and 'Blot'. The anisotropy for the effective thermal conductivity is much smaller than the anisotropy of the microstructure. This result is directly linked to the fact that the contrast between the intrinsic thermal conductivities of both phases (fibres and pores) is relatively small.

Figure 6 also shows that all the components of the effective thermal conductivity tensor reach an asymptotic value when the length L is larger than 200 to 300 µm (around 10 L_{cx} or L_{cy}). Once again, we consider effective thermal conductivity of the whole bulk as the reference. Therefore if we consider a volume (10 Lc_x x 10 Lc_x x 35 µm), the relative error made on thermal conductivity measurement is less than 2% for 'Blot' and 'Hard'.

Permeability

Figure 7 presents the evolution of the diagonal components of the permeability tensor of both samples versus the length L of the volume. The non-diagonal components of the permeability tensor are negligible and therefore are not presented here.

The permeabilities k_{xx} and k_{yy} are of the same order of magnitude whereas the transversal one, k_{zz}, is smaller. These results show that the permeability tensor is also transverse isotropic. The ratio k_{xx}/k_{zz} (or k_{yy}/k_{zz}) measures the anisotropy of the permeability tensor. This ratio is equal to 4 and 2.2 for 'Hard' and 'Blot', respectively, i.e. smaller than the anisotropy of the microstructure and larger than the anisotropy of the effective thermal conductivity.

Figure 7 also shows that the diagonal components of the permeability tensor reach an asymptotic value when the length L is larger than 400 µm (about 14 Lc_x or Lc_y). By using the permeability of the whole bulk as a reference, we can evaluate the relative error made on the permeability measurement if we consider a volume (10 Lc_x x 10 Lc_x x 35 µm). The maximum relative error is about 20% for 'Hard' and 'Blot', depending on the component. Note that this relative error is less than 10% if we consider a larger volume: (15 Lc_x x 15 Lc_x x 35 µm)

DISCUSSION OF THE REV SIZE

Sample Scale

Regardless of the property studied, the evolution of the curves as a function of the length L presents similar behaviour. For

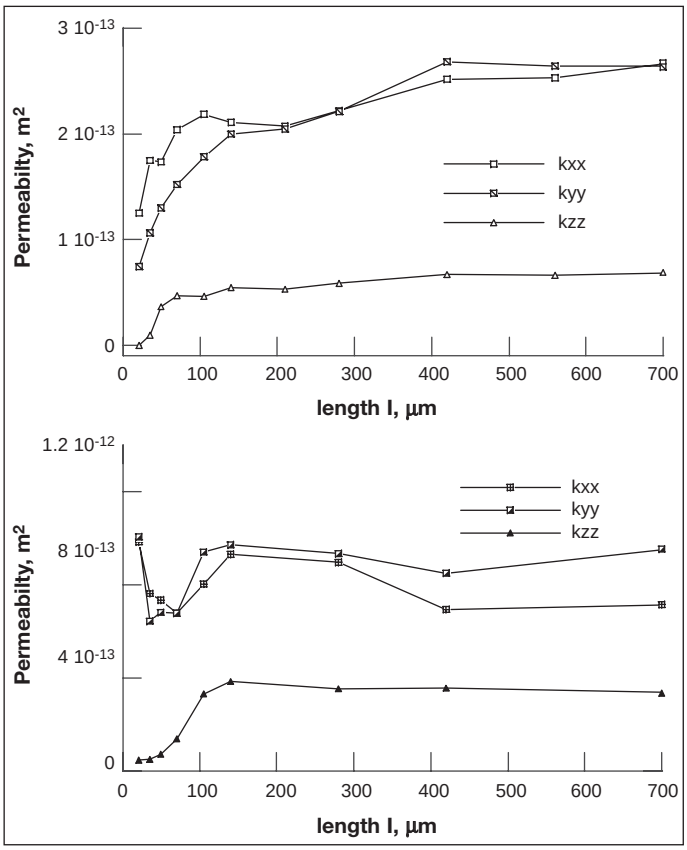

Fig. 7 Evolution of the principal components of the permeability tensor versus the (size) side L of the volume (L x L x 35 µm³) in the bulk for 'Hard' (top) and 'Blot' (bottom).

Table 2
Structural results obtained at the floc scale. L_{cx} and the specific surface area are expressed in µm and in m^{-1}, respectively.

Property	Lc_x	Porosity	Specific surface area
Mean	26	0.53	151000
Standard deviation	+/-4.2	+/-0.03	+/-33000

Table 3
Structural results obtained at the A4 scale. L_{cx} and the specific surface area are expressed in µm and in m^{-1}, respectively.

Property	Lc_x	Porosity	Specific surface area
Mean	32	0.47	102000
Standard deviation	+/- 4.2	+/-0.03	+/-33000

small volumes, they vary and then stabilise at a length of about 200 to 400 microns. The results show that the REV sizes lie between 5 and 15 times the heterogeneity length. If we consider a representative volume of 10 L_{CX}, the error made on property measurement is smaller than 5% for the porosity, the specific surface area and the effective thermal conductivity and up to 20% for the permeability. Finally note that the influence of thickness on the microstructural and physical properties measurements of the two papers has been also investigated. These results are not presented here, but in summary it appears that the chosen thickness of 35 microns is also representative.

Larger scales

The heterogeneity lengths for paper containing fillers have been evaluated by one of the authors (Rolland du Roscoat (*11*)) and from those results it appears that this length is not affected by the presence of fillers and that the REV for microstructural properties is also not affected. Hence, although the following preliminary results at larger scale were carried out on a printing paper (containing fillers) we believe they can also apply to a non-filled pure cellulose paper. Two scales are considered. The first one is the floc scale. In a square of 2 cm^2, 5 non overlapping samples were extracted and imaged. The results are presented in Table 2. We also imaged 20 samples randomly extracted from the same sheet of an A4 size. (Table 3).

These tables indicate that the mean values of the three main structural characteristics are of the same order of magnitude regardless of scale. The difference between the two tables can be explained from the fact that the data in Table 2 are located in a floc whereas table 3 refers to the whole paper sheet.

CONCLUSION

We have presented tools to characterise the properties of two paper samples imaged by Synchrotron X-ray microtomography coupled with analysis tools. Both microstructural characteristics and numerically evaluated physical properties were studied. Special attention has been paid to the determination of the Representative Elementary Volume, for both microstructural and physical properties for a given thickness in the bulk. We find that all the REV sizes lie between 5 and 15 times the covariance length (Lc_x or Lc_y) i.e., the heterogeneity length, with a reasonable accuracy. It appears that a volume of about (400 µm x 400 µm x 35 µm) can be considered as a representative volume for all the properties studied. It is smaller that the volume imaged (1400 µm x 1400 µm x paper_thickness) and is much smaller than the typical sizes of a paper sheet.

REFERENCES

(*1*) Ramaswamy S., Huang S., Goel A., Cooper A.,Choi D., Bandyopadhyay A., and Ramarao B.V. – The science of paper making, *12th Fundamental research Symposium*, Oxford, UK, 2:1289 (2001).

(*2*) Ramaswamy S., Gupta M., Goel A., Aaltosalmi U., Kataja M., Koponen A. and Ramarao B.V. – *Colloids and Surfaces A: Physicochemical and Engineering Aspects*, **241**:323 (2004).

(*3*) Ostoja-Starzeski M., Probabilistics Engineering mechanics, **21**:112 (2006).

(*4*) Rolland du Roscoat S., Decain M., Thibault X., Geindreau C. and Bloch J.-F., – *Acta Materialia* **55**:2841 (2007).

(*5*) Rolland du Roscoat S., Thibault X. and Bloch J.-F – *Journal of physics D: Applied physics*, **38**:A78 (2005)

Continued on Page 301

angle for R10 decreased differently from the water repellency classification, suggesting that the contact angle is not a reasonable method to evaluate water repellency of a highly water-resistant paperboard. Therefore it could be concluded that both the Stöckigt sizing test and the contact angle test are not suitable to estimate water repellency characteristics of paperboard in short time.

Finally, it seems obvious that the computerized measuring method of water repellency degree is the simplest method to define water resistance of paperboard specimens with high grammage (more than 200 gsm) in a short time.

CONCLUSIONS

The traditional test method for measuring the water repellency of paper and paperboard can be influenced by an operator's bias. In order to remove such bias, an automatic analysis program to assess water repellency was developed based on the different shape features of the liquid traces formed on paper specimens. Through the shape recognition principle of a liquid track flowing down the specimen at an angle of 45°, the unique features of the liquid tracks, such as the widths between the heads and tails of the traces (S_{HT}), the uniformity of liquid flow (S_d), the length of long traces (L_{ST}) and the eccentricity of liquid traces (E_i) were analyzed to determine the specific degree of water repellency. Finally, a novel method for the analysis of water repellency was developed, based on the shape recognition method, which made it possible to readily measure the water resistance of paper and paperboards and classify them into categories from R0 to R10.

REFERENCES

(*1*) Niskanen K. – **Paper Physics**, Papermaking Sci. and Tech. Vol.16, PI & TAPPI Press, Finland (1998).

(*2*) Neimo N. – **Papermaking Chemistry**, Papermaking Sci. and Tech. Vol.4, PI & TAPPI Press, Finland (1998).

(*3*) Neimo L. – Measurement of the hydrophobicity of paper, Paper Science Centre Communication No. 61, KCL, Finland, 1994, 45 pp.

(*4*) Kumler R.W. – "Testing paper and board for sizing" in **The Sizing of Paper** (W.F. Reynolds, Ed.) TAPPI PRESS, Atlanta, 1989, p. 103.

(*5*) Kurrle F.L., "Sizing test methods," TAPPI 1987 Sizing Short Course Notes, TAPPI PRESS, Atlanta, p. 9.

(*6*) KS M 7057 – Testing Method for Water Repellency of Paper and Paperboard.

(*7*) JIS P 8137 – Testing method of water repellency of paper and paperboard (nullified in 1998).

(*8*) Otsu N. – A Threshold Selection Method from Gray-Level Histograms, *IEEE Trans. Systems, Man and Cybernetics*, 9: 62-66 (1979).

(*9*) Ray B.K. and Ray K.S. – Corner detection using iterative Gaussian smoothing with constant window size, *Pattern Recognition*, **28**(11):1765-1781 (1995).

(*10*) Li J.C. and Schenk A.F. – Aerial Image Matching Using PSI-S Representation, Project Report No. 1 in Photogrammetry, Dept. of Geodetic Science, OSU (1989).

(*11*) Kass M., Witkin A. and Terzopoulos D. – Snake: Active Contour Models, *Intl. J. of Computer Vision*, 321-331 (1988).

(*12*) Geiger Davi., Gupta A., Costa L.A. and Vlontzos J. – Dynamic Programming for Detecting, Tracking and Matching Deformable Contours, *IEEE Trans. on PAMI*, **17**(3):284-302 (1995).

Original manuscript received 5 February 2007, revision accepted 6 November 2007.

Continued from page 290

(*6*) T. Kanit, S. Forest, I. Galliet, V. Mounoury, and D. Jeulin. – Determination of the size of the representative volume element for random composites: statistical and numerical approach. *Intl J.*, **40**:3647–3679, 2003.

(*7*) Drugan, W.J.; Willis, J.R., W. Drugan and J. Willis. – A micromechanics-based nonlocal constitutive equation and estimates of representative volume element size for elastic composites. *Journal of the mechanics and physics of solids*, **44**(4):497–524, 1996.

(8) Auriault J.L. and Ene H. – Macroscopic Modelling of Heat Transfer in Composites with Interfacial Thermal Barrier *Int. J. Heat Mass Transfer*, **37**:2885-2892, 1994.

(*9*) Bernard D, Nielsen Ø., Salvo L., Cloetens P. – Permeability assessment by 3D interdendritic flow simulations on microtomography mappings of Al–Cu alloys *Materials Science and Engineering A*, **392**:112–120, 2005

(*10*) Wiegmann A. and Zemitis A., – Simulation of Thermal, Proc. conductivity, diffusivity and electric force fields Workshop on Microstructure Simulation and Virtual Material Design, Kaiserslautern (2006)

(*11*) Rolland du Roscoat S. - **Contribution à la quantification 3D de réseuax fibreux par microtomographie à rayonnement synchrotron : application aux papiers,** PhD thesis, Institut National Polytechnique de Grenoble, France, 2007.

Original manuscript received 25 July 2007, revision accepted 12 December 2007